

Supporting Information

Writing and Erasing Multicolored Information in Diarylethene-Based Supramolecular Gels

Chien-Wei Hsu, Claire Sauvée, Henrik Sundén, and Joakim Andréasson**

Chalmers University of Technology, Department of Chemical and Chemical Engineering,
Chemistry and Biochemistry, Kemivägen 10, 412 96, Göteborg, Sweden
E-mail: sundenh@chalmers.se, a-son@chalmers.se

A. General Information

B. SEM imaging of OTHO3 gel

C. Rheology Measurements

D. Photophysical Measurements

E. Energy Transfer Mechanisms

F. Irradiation wavelength selection and isomerization efficiencies

G. References

A. General Information

All reagents and solvents were purchased from Sigma-Aldrich, Alfa Aesar and TCI and used without any further purification unless specified notice. NMR spectra were acquired on an Agilent 400 MHz NMR machine at 25 °C. Mass spectrometry measurements were performed at the Department of Chemistry and Chemical Engineering, Chalmers University of Technology. SEM imagings were taken on a FEI Quanta200 ESEM.

Materials

9,10-Diphenylanthracene (DPA) dye:
DPA was purchased from Sigma-Aldrich.

DAE photoswitches:
The synthetic procedure followed previous literature. NMR spectra matched reported data.^{[1][2]}

Gelator-OTHO3:
The synthesis followed established procedures from our group.^{[3][4]}

B. SEM imaging of OTHO3 gel

SEM pictures were taken on a FEI Quanta200 ESEM. The gels were left in open vials to dry for 1 week and Scanning Electron Microscopy (SEM) was performed on the obtained xerogels.

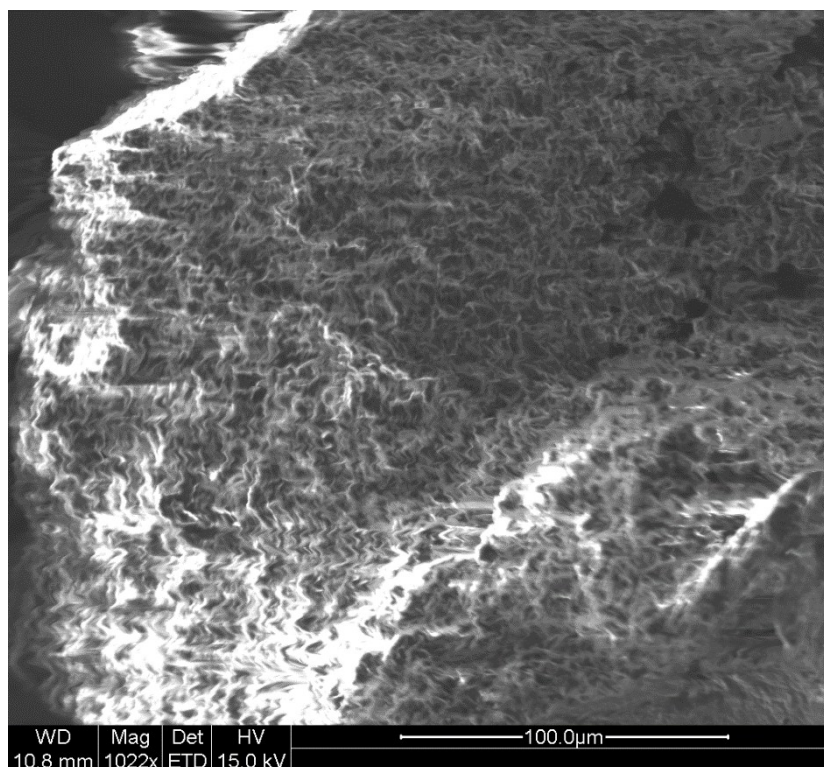


Figure S1. SEM imaging of OTHO3 in toluene (1.5 wt%). Scale bar: 100 μm.

B. Rheology Measurements

The rheological properties of the gels were determined using a DHR-3 (TA instruments) with a parallel plate and plate geometry. The plate had a diameter of 40 mm and a gap of 50 μm . The bottom plate was sandblasted. To reduce evaporation, the measurements were performed in a closed atmosphere and the cone was equipped with a solvent trap. The temperature was controlled using a Peltier plate. The strain was set to 0.5% for all measurements except the strain step that was performed at 0.5 and 40%. The frequency was set to 6.28 rad/s except for the frequency sweep which was performed between 0.02 and 100 rad/s.

Two gels were compared using dynamic shear oscillation, one gel of gelator OTHO3 at 20 mM in toluene and one gel of gelator OTHO3 (20 mM), DPA (6×10^{-4} M), DAE-5 (3×10^{-3} M) and DAE-8 (3×10^{-3} M). Frequency sweeps (a) show that G' is about one order of magnitude larger than G'' for both gels, which is characteristic of LMWG. The gel strength is reduced in the gel containing all compounds. Repeated strain steps (b) onto the gels showed that both gels exhibit liquid moduli at higher strains (grey) and reform into a gel with a lower strain (white).

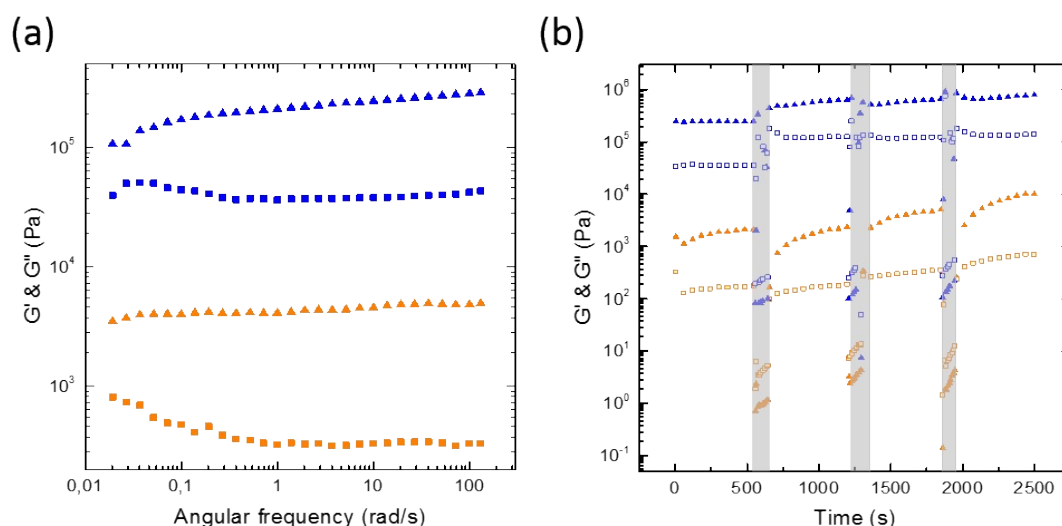


Figure S2. (a) Storage (triangle) and loss (square) moduli of sugar gel alone (blue) and sugar gel+DPA+DAE5+DAE8 (orange) as a function of frequency. (b) Storage (triangle) and loss (square) moduli of sugar gel alone (blue) and sugar gel +DPA+DAE5+DAE8 (orange), step-strain measurement, at a strain of 0.05 % (white areas) and a strain of 40 % (grey area) and a frequency of 6.28 rad/s

C. Photophysical Measurements

The preparation of samples was in a dark room to avoid the isomerization reactions. Firstly the dyes, gelator and solvent were added into a 4 mL vial and gently heated until all the compounds dissolved. Then the mixture solution was transferred to a quartz cuvette. Sonication for 10 minutes was needed if the mixture solution did not form a gel.

All the measurements were performed at 1 atm and room temperature, unless specifically noted. Ground state UV-Vis absorption spectra were recorded on a Cary 5000 UV/Vis spectrometer. Steady-state emission spectra were recorded on a SPEX Fluorolog-3 spectrofluorimeter.

Fluorescence lifetimes measurements were performed using time correlated single photon counting (TCSPC) setup. The excitation light was provided at a repetition rate of 10 kHz by a 377 nm diode laser (LDH-P-C-375) powered by a PDL-800B pulsed diode driver (Picoquant, GmbH Germany). The emitted photons were collected at the magic angle (54.7°) at 410 nm and 530 nm alternatively by a thermoelectrically cooled microchannel plate photomultiplier tube (R3809U-50, Hamamatsu). The signal was digitalized using a multi-channel analyzer with 2048 channels (SPC-300, Edinburgh Analytical Instruments) and to ensure good statistics 10000 counts were recorded in the top channel. The measured fluorescence decays were fitted using the program FluoFit Pro v.4 (PicoQuant GmbH, Germany) after deconvolution of the data with the instrument response function (IRF) with FWHM~40 ps. The quality of the fit was assessed by minimizing the reduced χ^2 function and by visual inspection of the weighted residuals.

Isomerization reactions.

The photoinduced isomerization reactions of DAE were performed under the irradiation of a UVP lamp model UVGL-25 (365 nm, 1.5 mW/cm²) or a 450 W xenon arc lamp from the SPEX Fluorolog-3 (the selected wavelength was tuned by the monochromator).

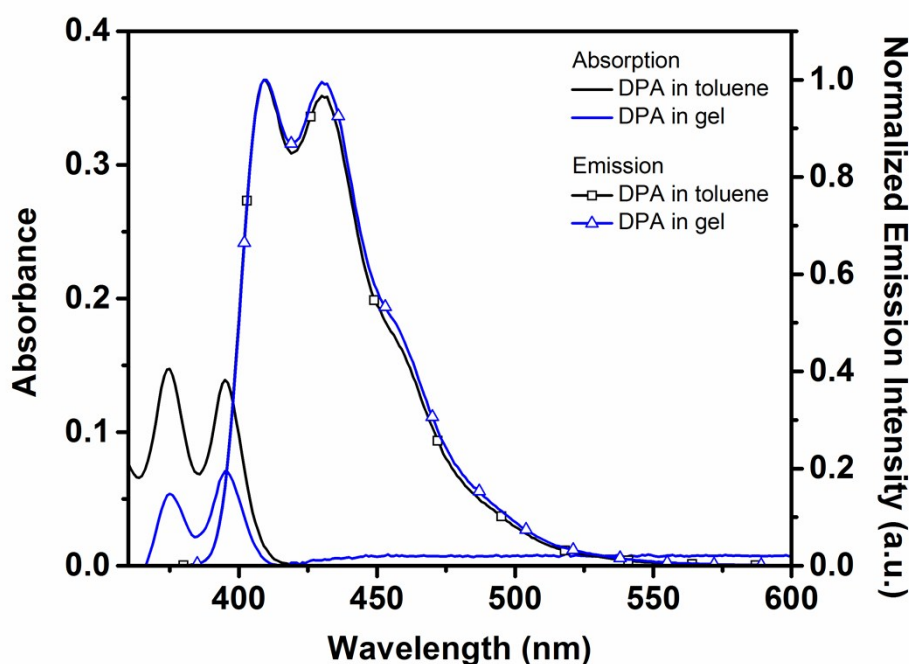


Figure S3. UV-Vis absorption and fluorescence spectra of DPA (10^{-6} M) in toluene and in gel. The gel concentration is 20 mM in toluene.

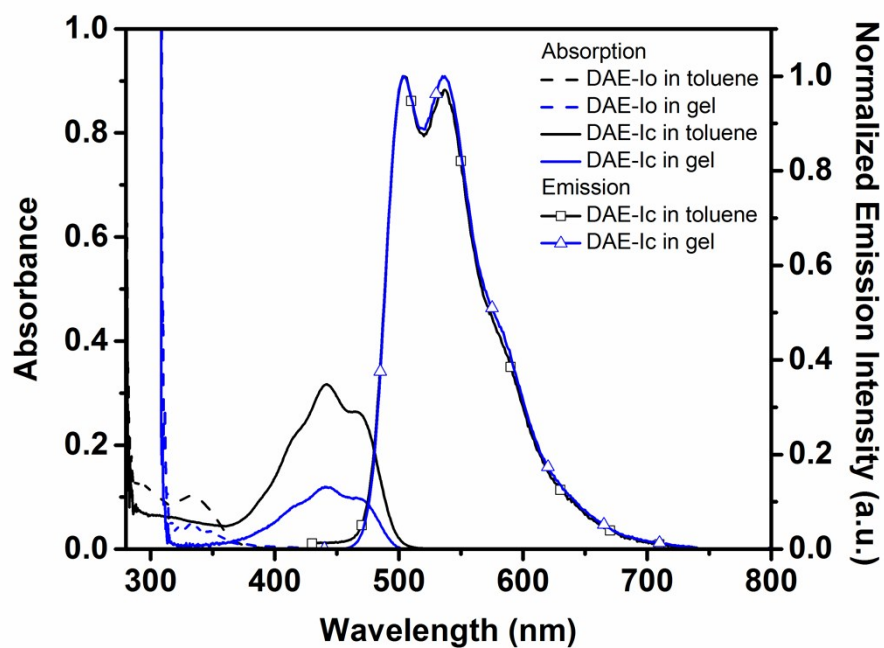


Figure S4. UV-Vis absorption and fluorescence spectra of DAE-I (10^{-5} M) in toluene and in gel. The gel concentration is 20 mM in toluene.

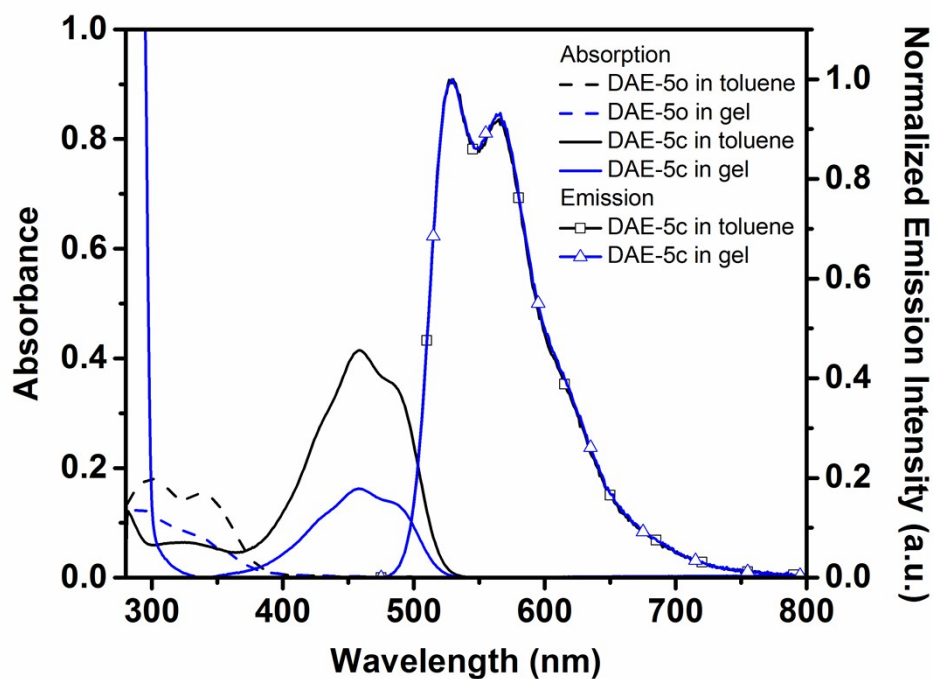


Figure S5. UV-Vis absorption and fluorescence spectra of DAE-5 (10^{-5} M) in toluene and in gel. The gel concentration is 20 mM in toluene.

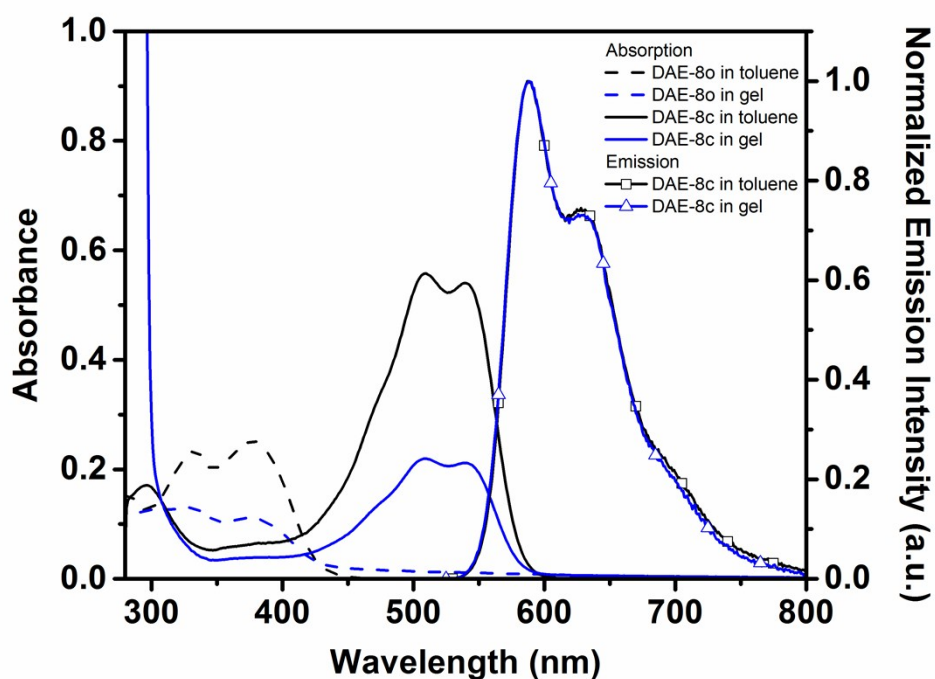


Figure S6. UV-Vis absorption and fluorescence spectra of DAE-8 (10^{-5} M) in toluene and in gel. The gel concentration is 20 mM in toluene.

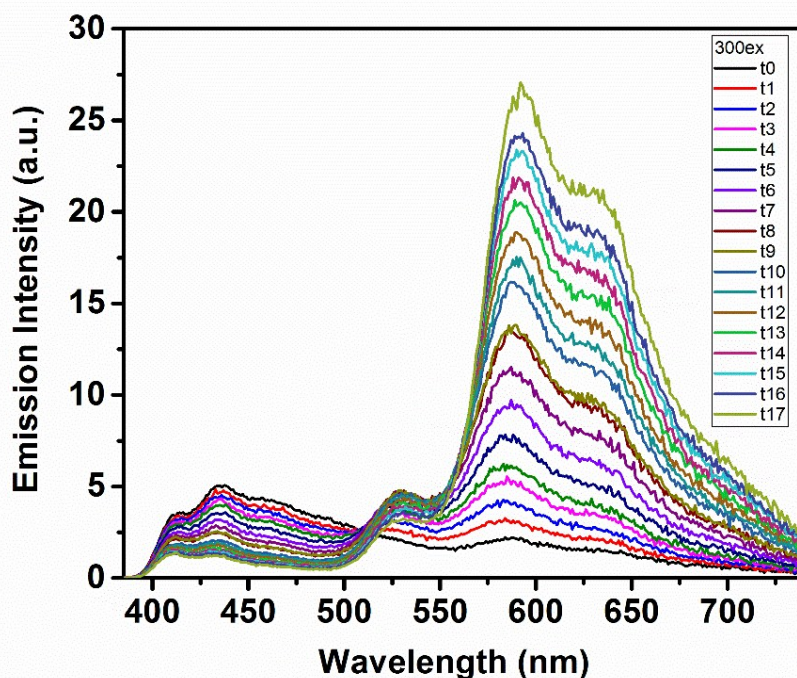


Figure S7. Fluorescence spectra of the mixture DPA/DAE-5/DAE-8 in OTHO3 gel at different degrees of light-induced isomerization. $\lambda_{\text{ex}} = 300$ nm. The concentration of DPA is 6×10^{-4} M, DAE-5 is 3 mM and DAE-8 is 2 mM, and OTHO3 gelator is 20 mM in toluene. $t_0 = 0$ s, $t_{17} = 2610$ s, total irradiation time 2610 s.

E. Energy Transfer Mechanisms

Given the concentrations of the energy donor (DPA) and the corresponding acceptors (DAEs) we consider two main excitation energy transfer (EET) mechanisms: Radiative “trivial” EET and FRET-type EET. The latter acts at donor-acceptor distances on the order of the critical Förster radius R_0 or shorter (for DPA and DAE-5 around 50 Å) and is manifested in a decreased lifetime of the donor, while the former does not depend on the donor-acceptor distance and the donor lifetime is not expected to change.

For the concentrations used in the bi-component systems in Figures 3a-c ($[DPA]=10^{-5}$ M, $[DAE]=10^{-4}$ M) the average nearest-neighbor distance is around 13 nm. This implies that the major EET contribution is ascribed to radiative EET. This notion is supported by time-resolved single photon counting (SPC) experiments. DPA alone has a lifetime of 5.4 ns, whereas it displays a bi-exponential decay with lifetimes $\tau_1=5.5$ ns (78%) and $\tau_2=1.2$ ns (22%) in a gel containing 600 μ M DPA and 250 μ M DAE-5. We assign the short-lived component to EET quenching by the FRET-mechanism, and hence, the main EET contribution stems from radiative EET as the observed overall quenching of DPA emission in the gels is too efficient to be explained only by the relatively small FRET-contribution. In the tri-component systems in Figure 3d, the concentrations are increased to $[DPA]=600$ μ M, $[DAE-5]=[DAE-8]=3$ mM. Here, the average nearest-neighbor distance is around 4 nm, and we would thus expect a much larger contribution from FRET-type EET. Indeed, this is supported by the SPC measurements in which DPA displays a bi-exponential decay with $\tau_1=2.4$ ns (48%) and $\tau_2=0.9$ ns (52%). In the SPC experiment, $[DPA]=600\mu$ M and $[DAE-5]=6$ mM.

F. Irradiation wavelength selection and isomerization efficiencies.

For the gels containing only one DAE derivative (Figures 2b-f and Figures 3a-c), selective isomerization is not an issue, as there is only one DAE derivative to be isomerized. Hence, the irradiation wavelength for isomerization is of no importance as long as the UV light is being absorbed by the open isomer. Here, we chose the hand held UVP lamp model UVGL-25 (365 nm, 1.5 mW/cm²). For the gels containing two DAE derivatives (DAE-5 and DAE-8, Figure 3d), selective isomerization from the open to the closed form is key to the function. DAE-8o is virtually the exclusive absorber at 425 nm, why this wavelength was chosen for the isomerization DAE-8o→DAE-8c.

There is no wavelength at which DAE-5o is the exclusive absorber. Furthermore, the isomerization quantum yields open→closed are not very different for DAE-5 and DAE-8 in non-polar solvents (0.42 and 0.21 for DAE5 and DAE-8, respectively, in 1,4-dioxane)¹. However, in polar milieus the isomerization efficiency DAE-8o→DAE-8c is dramatically reduced as a donor (thiophene) – acceptor (sulfone) interaction suppresses the closing reaction. This is why irradiation at 300 nm mainly will induce the much more efficient isomerization reaction DAE-5o→DAE-5c rather than DAE-8o→DAE8c.

As for the opening reactions DAEc→DAEo, the isomerization quantum yields are dramatically lower than the closing reactions (closing reactions: 0.42 and 0.21 for DAE-5 and DAE-8. Opening reactions: 4.0×10^{-4} and $<1.0\times 10^{-5}$ for DAE-5 and DAE-8)¹. This implies that the wavelength of the isomerization light used to trigger the opening reactions must be chosen so that it does not overlap with the absorption spectra of the open isomers. The visible light

LEDs used in our laboratory has a FWHM of 20 nm at best, why we chose to use an LED at 523 nm for the isomerization reaction DAE-5c→DAE-5o (Figure 2c). An obvious and advantageous effect of the much lower isomerization quantum yields for the opening reactions is that 100% enrichment in the closed isomeric form is easily achieved using any irradiation wavelength in the UV region absorbed by the open isomers.

G. References

1. K. Uno, H. Niikura, M. Morimoto, Y. Ishibashi, H. Miyasaka, M. Irie, *J. Am. Chem. Soc.* 2011, **133**, 13558-13564.
2. F. Gillanders, L. Giordano, S. A. Díaz, T. M. Jovin, and E. A. Jares-Erijman, *Photochem. Photobiol. Sci.*, 2014, **13**, 603-612
3. A. Axelsson, L. Ta, and H. Sundén, *Eur. J. Org. Chem.*, 2016, **20**, 3339-3343.
4. C. Sauvée, A. Ström, M. Haukka, and H. Sundén, *Chem. Eur. J.*, 2018, **24**, 8071-8075.